Supplementary material

S1. Details of the study area

Water bodies such as estuaries, channels, and creeks comprise almost 19% of the total area of the Indian Sundarban Biosphere Reserve (9600 km^2), and the remaining area consists of an archipelago of 102 islands, 54 of which have human habitation. At present, the Hooghly River is the only perennial freshwater input to the Sundarbans, with an annual water discharge of 8.3×10^{10} m^3 (Samanta et al., 2015); however, it flows along the western margin of the Sundarban mangroves. The rest of the rivers – namely the Saptamukhi, Thakuran, Matla, Bidya, and Gosaba – act as arms of the sea (or tidal inlets), because the freshwater influx from the perennial flow of the Hooghly River is blocked upstream by siltation (Akhand et al., 2016; Sarkar et al., 2004).

The estuaries of the Sundarbans are categorized as meso-macro tidal (having a neap-to-spring variation in tidal amplitude of >1.5 m to <5 m) with semidiurnal tidal cycles (Chatterjee et al., 2013). Atmospheric conditions in this part of the world are mostly unstable throughout the year with high wind velocity, which in turn facilitates intensive vertical mixing of the water column (Goutam et al., 2015, Sadhuram et al., 2005). Mean current velocities range between 108 and 117 cm s^{-1} during flood and ebb tides, respectively (De et al., 2011).

This region experiences an annual mean rainfall of 1973 mm, which acts as an additional freshwater input; however, the majority of this rainfall occurs in the monsoon season, i.e. between June and September (Ray et al., 2013). The present study was conducted in the waterways adjacent to Dhanchi Island, which shelters dense mangrove

patches containing species such *Avicennia marina*, *A. alba*, and *A. officinalis* in abundance. Species such as *Ceriops decandra*, *Excoecaria agallocha*, *Phoenix paludosa*, and *Bruguiera gymnorrhiza* are found in scattered patches.

References

Akhand, A., Chanda, A., Manna, S., Das, S., Hazra, S., Roy, R., Choudhury, S.B., Rao, K.H., Dadhwal, V.K., Chakraborty, K., and Mostofa, K.M.G., Tokoro, T., and Kuwae, T.: A comparison of CO_2 dynamics and air-water fluxes in a river-dominated estuary and a mangrove-dominated marine estuary, Geophys. Res. Lett., 43(22), 11–726, https://doi.org/10.1002/2016GL070716, 2016.

Chatterjee, M., Shankar, D., Sen, G.K., Sanyal, P., Sundar, D., Michael, G.S., Chatterjee, A., Amol, P., Mukherjee, D., Suprit, K., and Mukherjee, A.: Tidal variations in the Sundarbans estuarine system, India, J. Earth Syst. Sci., 122(4), 899–933, https://doi.org/10.1007/s12040-013-0314-y, 2013.

De, T.K., De, M., Das, S., Chowdhury, C., Ray, R., and Jana, T.K.: Phytoplankton abundance in relation to cultural eutrophication at the land-ocean boundary of Sunderbans, NE Coast of Bay of Bengal, India, J. Environ. Stud. Sci., 1(3), 169, https://doi.org/10.1007/s13412-011-0022-3, 2011.

Goutam, K.S., Tanaya, D., Anwesha, S., Sharanya, C., and Meenakshi, C.: Tide and Mixing Characteristics in Sundarbans Estuarine River System, Hydrol. Curr. Res., 6(2), 1, 2015.

Ray, R., Chowdhury, C., Majumder, N., Dutta, M.K., Mukhopadhyay, S.K., and Jana, T.K.: Improved model calculation of atmospheric CO_2 increment in affecting carbon

stock of tropical mangrove forest, Tellus B: Chem. Phys. Meteorol., 65(1), 18981, https://doi.org/10.3402/tellusb.v65i0.18981, 2013.

Sadhuram, Y., Sarma, V.V., Murthy, T.R., and Rao, B.P.: Seasonal variability of physico-chemical characteristics of the Haldia channel of Hooghly estuary, India, J. Earth Syst. Sci., 114(1), 37–49, https://doi.org/10.1007/BF02702007, 2005.

Samanta, S., Dalai, T.K., Pattanaik, J.K., Rai, S.K., and Mazumdar, A.: Dissolved inorganic carbon (DIC) and its $\delta^{13}C$ in the Ganga (Hooghly) River estuary, India: Evidence of DIC generation via organic carbon degradation and carbonate dissolution, Geochim. Cosmochim. Acta, 165, 226–248, https://doi.org/10.1016/j.gca.2015.05.040, 2015.

Sarkar, S.K., Frančišković-Bilinski, S., Bhattacharya, A., Saha, M., and Bilinski, H.: Levels of elements in the surficial estuarine sediments of the Hugli River, northeast India and their environmental implications, Environ. Int., 30(8), 1089–1098, https://doi.org/10.1016/j.envint.2004.06.005, 2004.

S2. Computation of net ecosystem productivity (NEP) and net ecosystem calcification (NEC) rates

To evaluate the effect of biological processes such as net ecosystem productivity (NEP) and net ecosystem calcification (NEC) on estimated total alkalinity (TAlk) and dissolved inorganic carbon (DIC), TAlk and DIC over a complete diel cycle were computed by equilibrium calculations using CO_2SYS software and the measured pH and pCO_2(water). We then quantified the TAlk and DIC budget change per unit area. We eliminated the effect of freshwater mixing with river water on TAlk and DIC at the sampling sites by calculating the difference between measured TAlk and DIC and the conservative-mixing values (ΔTAlk and ΔDIC). Conservative-mixing values were calculated as the linearly interpolated value between two end-members – a freshwater end-member (FWEM) and a marine end-member (MEM) – on a plot of salinity vs. TAlk or salinity vs. DIC.

Next, the raw value of the budget change per unit area (*budget_raw*) was calculated as the change rate of ΔTAlk and ΔDIC per minute divided by the water depth, according to the equation

$$budget\_raw_i = (TAlk_{i+1} \; or \; DIC_{i+1} - TAlk_i \; or \; DIC_i)/sampling\_interval/$$

$$water\_depth_i \hspace{6cm} (\text{S1})$$

where i is the measurement time. The sampling interval was 2 min. The raw values of the budgets showed extreme fluctuations due to the differences in the time response and the measurement distance of the pH and pCO_2 sensors. Such fluctuations were thought to occur over a period shorter than several minutes, and real-time ecosystem changes should occur over a longer period. Thus, we applied a low-pass filter using an exponential moving average as follows to remove the short-period fluctuations from the ecosystem activities occurring over a longer period.

$$budget_i = (1 - A) \times budget_{raw_i} + A \times budget_{i-1}. \qquad \text{(S2)}$$

$$A = exp(-1/(t \times s)) \qquad \text{(S3)}$$

$$budget_0 = 0 \qquad \text{(S4)}$$

where t is the time constant and s is the measurement frequency (=1/60 Hz). Most of the variability at frequencies longer than 10 times the time constant will remain (>99%), whereas most of the variability at frequencies less than one-tenth of the time constant will be removed (<1% remaining) (Moore, 1986). In this study, we set the time constant to 8640 s, which means that more than 99% of the data showing patterns at one diurnal cycle or longer (24 h = 86,400 s) remained, whereas more than 99% of data showing cycles of several to 10 min (>864 s ≈ 15 min) was eliminated.

When the budgets can be explained exclusively by major biological processes such as NEP and NEC, these can be quantified as follows (Zeebe and Wolf-Gladrow, 2001; Tokoro et al. 2014):

$$NEP = -budget_{DIC} + 0.5 \times budget_{TAlk} \qquad (S5)$$

$$NEC = -0.5 \times budget_{TAlk} \qquad (S6)$$

We evaluated whether the budgets at each site could be explained by NEP or NEC by fitting both NEP and NEC data to the irradiance–ecosystem activities curve, assuming that the effect of temperature was negligible (temperatures varied within a narrow range; see 'Results' section 3.1 in the main text). For fitting the curve, the binned-average NEP and NEC were calculated at intervals of 100 μmol photon m^{-2} s^{-1}. We used the error range of the binned-averaged data (described below) for the weighted fitting. The irradiance curve used in this study was as follows (Jassby and Platt, 1976):

$$NEP = P_{max} \times tanh\left(\frac{\partial_P \times I}{P_{max}}\right) - R \qquad (S7)$$

$$NEC = C_{max} \times tanh\left(\frac{\partial_C \times I}{C_{max}}\right) - D \qquad (S8)$$

where P_{max} and C_{max} are the estimated maximum photosynthesis and calcification rates respectively. R and D are the estimated respiration and calcium carbonate dissolution rates, respectively. ∂_p and ∂_c are the initial slopes of the irradiance curves for photosynthesis and calcification, respectively.

Although, this equation is usually used for the photosynthetic activity of phytoplankton, to the best of our knowledge the fitting is also applicable to ecosystem

production and calcification because these metabolic responses to irradiance (e.g., directly proportional under low-light conditions and saturated under high-light conditions) can be approximated by a hyperbolic tangent curve. The values for the curve were determined by the weighted least-squares fitting method. If the P-value of the fit was greater than 0.05, then NEP and NEC at the site were not recognized as main factors affecting the TAlk and DIC budget change, and accordingly the calculated NEP and NEC were dismissed, given that parameters except for the irradiance (for example pore water or groundwater) were assumed to have negligible effect in this study. Daily NEP and NEC were calculated using the values from the irradiance–ecosystem activity curves.

References

Jassby, A.D., and Platt, T.: Mathematical formulation of the relationship between photosynthesis and light for phytoplankton, Limnol. Oceanogr., 21(4), 540–547, https://doi.org/10.4319/lo.1976.21.4.0540, 1976.

Moore, C.J.: Frequency response corrections for eddy correlation systems, Bound.-Layer Meteorol., 37(1–2), 17–35, https://doi.org/10.1007/BF00122754, 1986.

Tokoro, T., Hosokawa, S., Miyoshi, E., Tada, K., Watanabe, K., Montani, S., Kayanne, H., and Kuwae, T.: Net uptake of atmospheric CO_2 by coastal submerged aquatic vegetation, Glob. Change Biol., 20(6), 1873–1884, https://doi.org/10.1111/gcb.12543, 2014.

Zeebe, R.E. and Wolf-Gladrow, D.: CO_2 in Seawater: Equilibrium, Kinetics, Isotopes, Elsevier, Amsterdam, Netherland, 2001.

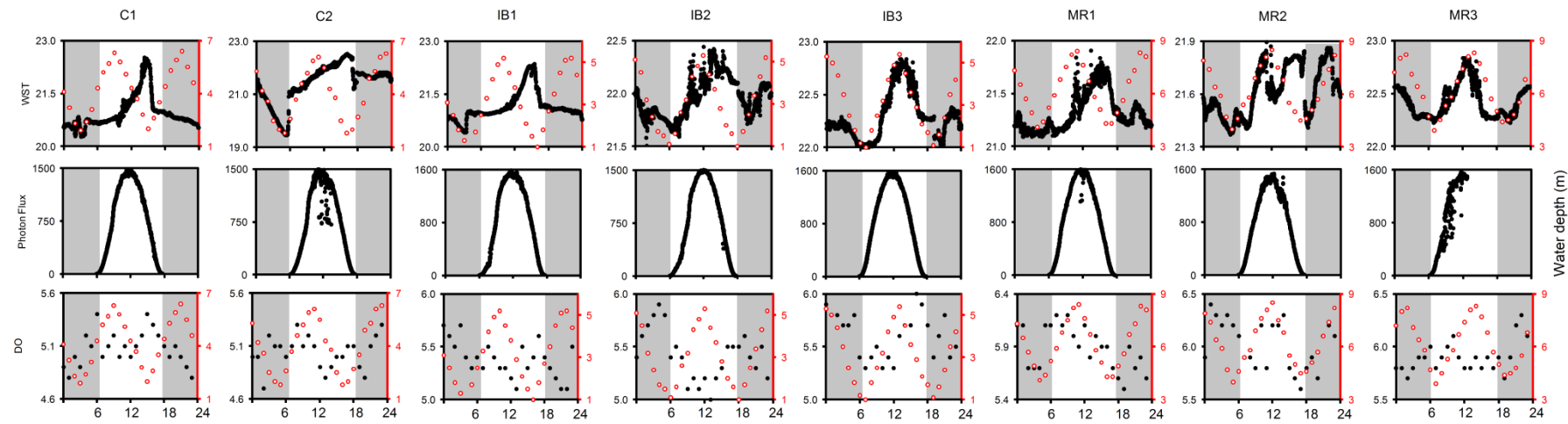**Figure S1.** Time-series plot of diel variation of water surface temperature (WST, °C), photon flux (μmol m^{-2} s^{-1}), and dissolved oxygen (DO, mg L^{-1}), at the (a) two creek stations (C1 and C2), (b) three island-boundary stations (IB1, IB2, and IB3), and (c) three mid-river stations (MR1, MR2, and MR3) along with the variation in water depth (metres, red circles and secondary *y*-axis). Peak high tide at C1 at 09:00 and 21:15 peak low tide at C1 at)3:30 and 15:00; peak high tide at C2 at 11:30 and 23:15; peak low tide at C2 at 05:30 and 17:00; peak high tide at IB1 at 10:00 and 21:30; peak low tide at IB1 at 04:00 and 15:45; peak high tide at IB2 at 00:30 and 12:00; peak low tide at IB2 at 06:30 and 18:00; peak high tide at IB3 at 00:30 and 13:00; peak low tide at IB3 at 07:00 and 18:30; peak high tide at MR1 at 10:30 and 22:00; peak low tide at MR1 at 04:00 and 16:30; peak high tide at MR2 at 10:00 and 22:30; peak low tide at MR2 at 04:30 and 16:00; peak high tide at MR3 at 00:30 and 13:00; peak low tide at MR3 at 07:00 and 18:30. All times are local time.
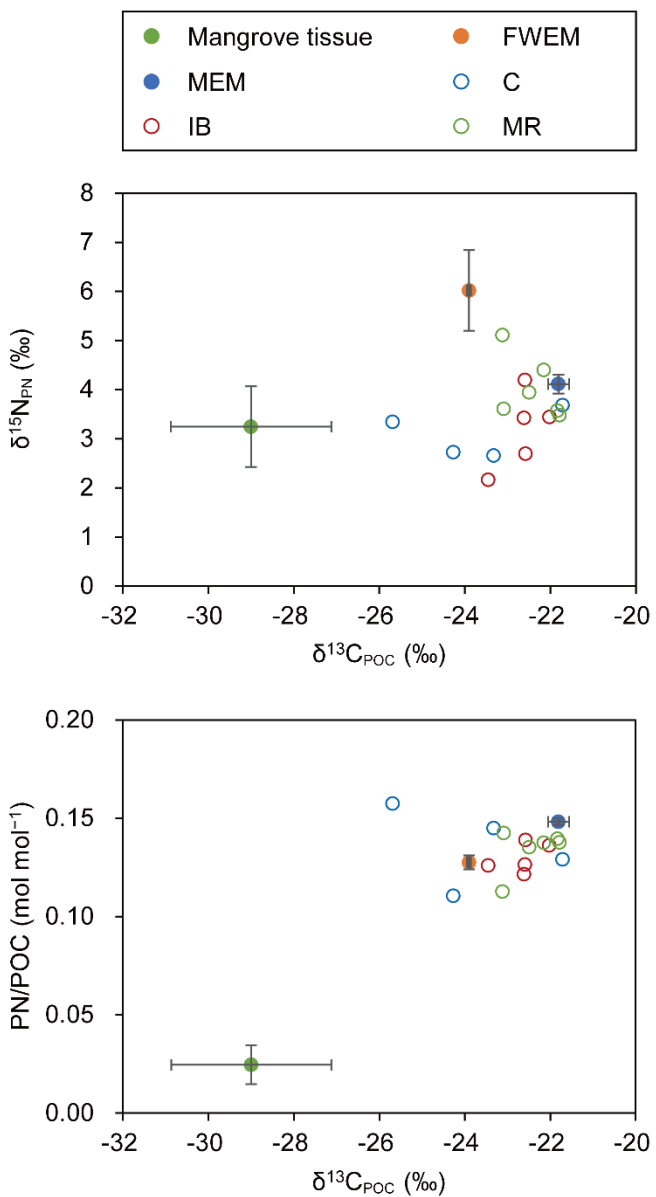
Figure S2. Isotopic and elemental signatures of organic matter sources and POM at the creeks (C), island boundary (IB) and mid-river (MR) adjacent to Dhanchi Island, Sundarban. Error bars show the standard deviations of each source.
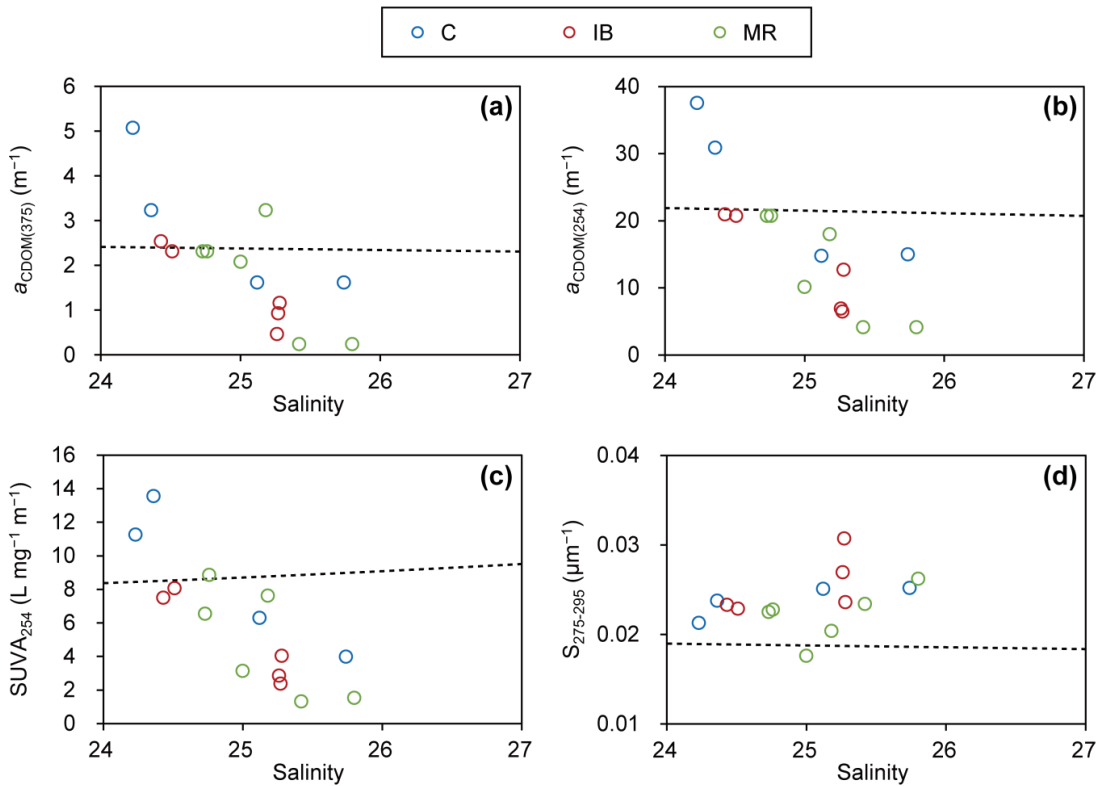
Figure S3. Distribution of (a) $a_{\text{CDOM}(375)}$, (b) $a_{\text{CDOM}(254)}$, (c) SUVA_{254}, and (d) $S_{275-295}$ as a function of salinity at creek (C), island-boundary (IB) and mid-river (MR) stations. The predicted two-end-member conservative-mixing distributions of the respective parameters are shown as the black dotted lines assuming the following values for the measured freshwater end-member (FWEM) and marine end-member (MEM): FWEM $a_{\text{CDOM}(375)} = 3.22 \text{ m}^{-1}$, MEM $a_{\text{CDOM}(375)} = 2.30 \text{ m}^{-1}$; FWEM $a_{\text{CDOM}(254)} = 30.86 \text{ m}^{-1}$, MEM $a_{\text{CDOM}(254)} = 20.73 \text{ m}^{-1}$; FWEM $\text{SUVA}_{254} = 2.62 \text{ L mg}^{-1} \text{ m}^{-1}$, MEM $\text{SUVA}_{254} = 0.95 \text{ L mg}^{-1} \text{ m}^{-1}$; FWEM $S_{275-295} = 0.023 \text{ µm}^{-1}$, MEM $S_{275-295} = 0.017 \text{ µm}^{-1}$.
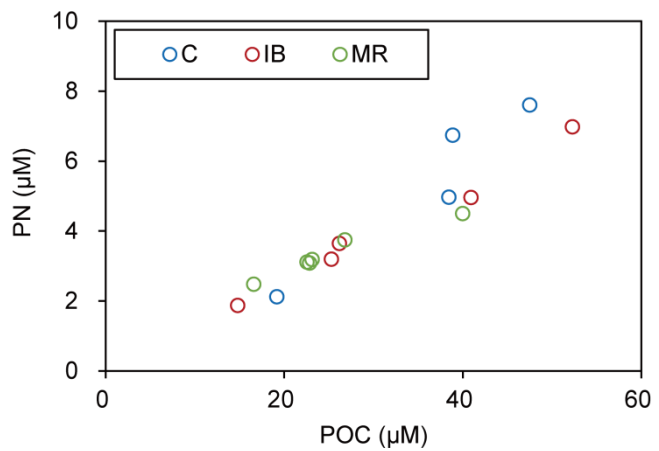
Figure S4. Relationship between particulate nitrogen (PN) and particulate organic carbon (POC) at creek (C), island-boundary (IB) and mid-river (MR) stations.

Table S1. Mean ± standard deviation and range (in parentheses) of all physico-chemical and carbonate-chemistry parameters measured at creek (C), island-boundary (IB) and mid-river (MR) stations.

Parameters	C	IB	MR
Water temperature (°C)	21.18 ± 0.66 (19.44–22.52)	21.79 ± 0.57 (20.41–22.83)	21.79 ± 0.49 (21.09–22.83)
Salinity	25.37 ± 0.65 (24.22–27.62)	21.79 ± 0.57 (20.41–22.83)	25.62 ± 0.35 (25.07–26.37)
Dissolved oxygen (mg L^{-1})	5.1 ± 0.2 (4.7–5.4)	5.5 ± 0.2 (5.0–6.0)	5.9 ± 0.2 (5.5–6.4)
pH	8.023 ± 0.015 (7.932–8.037)	8.032 ± 0.009 (7.936–8.056)	8.030 ± 0.002 (8.018–8.038)
Total alkalinity (μmol kg^{-1})	2047 ± 289 (1857–2683)	1936 ± 146 (1862–2372)	1887 ± 19 (1862–1911)
Dissolved inorganic carbon (μmol kg^{-1})	2219 ± 244 (2065–2732)	2112 ± 120 (2045–2471)	2078 ± 17 (2052–2099)
pCO_2(water) [μatm]	470 ± 162 (315–1204)	393 ± 48 (311–610)	380 ± 66 (320–636)
CO_2 flux (μmol m^{-2} h^{-1})	69 ± 181 (–104 to 887)	–17 ± 53 (–108 to 225)	–31 ± 73 (–99 to 251)
Revelle factor	12.0 ± 0.6 (11.0–14.1)	11.4 ± 0.3 (10.9–12.5)	11.7 ± 0.1 (11.5–12.2)
Photon flux (μmol m^{-2} s^{-1})	770.4 ± 516.8 (1.0–1535.0)	827.5 ± 559.0 (0.9–1583.7)	834.4 ± 549.5 (1.0–1608.0)
Dissolved organic carbon (μM)	103.9 ± 20.1 (82.4–136.1)	105.3 ± 20.3 (87.6–157.9)	104.2 ± 17.8 (84.7–148.9)
Particulate organic carbon (μM)	36.0 ± 12.0 (19.2–47.5)	31.9 ± 14.7 (14.8–52.3)	25.3 ± 7.9 (16.6–40.0)
Particulate nitrogen (μM)	5.3 ± 2.4 (2.1–7.6)	4.1 ± 1.9 (1.8–6.9)	3.3 ± 0.7 (2.5–4.5)
$\delta^{13}C_{POC}$ (‰)	–23.7 ± 1.6 (–25.6 to –21.7)	–22.6 ± 0.5 (–23.4 to –22.0)	–22.4 ± 0.6 (–23.1 to –21.8)
$\delta^{15}N_{PN}$ (‰)	3.1 ± 0.4 (2.6–3.6)	3.1 ± 0.7 (2.1–4.2)	4.0 ± 0.6 (3.5–5.1)
$\delta^{13}C_{DIC}$ (‰)	–3.4 ± 1.9 (–7.6 to –1.9)	–1.9 ± 0.2 (–2.3 to –1.6)	–2.2 ± 1.1 (–5.5 to –1.5)

Table S2. Mean ± standard deviation of TOC, TN, TOC:TN, δ^{13}C of TOC, and δ^{15}N of TN in the leaves of dominant mangrove species in the Indian Sundarbans.

Species name	TOC (%)	TN (%)	TOC:TN	δ^{13}C of TOC (‰)	δ^{15}N of TN (‰)
Avicennia marina	45.3 ± 0.6	1.6 ± 0.1	32.4 ± 3.1	–29.4 ± 0.1	4.1 ± 0.2
Excoecaria agallocha	44.8 ± 0.3	1.7 ± 0.1	29.9 ± 1.5	–26.1 ± 0.4	4.0 ± 0.1
Bruguiera gymnorrhiza	47.0 ± 0.7	0.6 ± 0.0	84.9 ± 5.1	–30.8 ± 0.9	2.3 ± 0.3
Phoenix paludosa	47.5 ± 1.3	1.6 ± 0.2	34.1 ± 3.6	–28.1 ± 0.4	3.3 ± 0.3

Table S3. Median and range of each OM source estimated using OM mixing model using three parameters (δ^{13}C, δ^{15}N and N:C). 95% credible interval is shown in parenthesis. C, creek; IB, island boundary; MR, mid-river.

	C	IB	MR
Relative contribution of mangroves	17% (2–44%)	11% (2% to 17%)	8% (1% to 14%)
Relative contribution of FWEM	23% (1% to 63%)	10% (0% to 47%)	9% (0% to 33%)
Relative contribution of MEM	56% (23% to 85%)	78% (47% to 88%)	83% (62% to 92%)

–

Table S4. Median and range of OM mixing model using two parameters (δ^{13}C and δ^{15}N). 95% credible interval is shown in parenthesis. C, creek; IB, island boundary; MR, mid-river.

	C	IB	MR
Relative contribution of mangroves	33% (6% to 69%)	9% (1% to 21%)	6% (0% to 17%)
Relative contribution of FWEM	16% (0% to 55%)	13% (0% to 46%)	9% (0% to 33%)
Relative contribution of MEM	46% (12% to 77%)	77% (48% to 91%)	83% (61% to 94%)